FLOW STRUCTURE NEAR THE LEADING EDGE OF A DEEP-WATER HYDRAULIC JUMP

Javier Rodríguez-Rodríguez, Alberto Aliseda and Juan C. Lasheras
Department of Mechanical and Aerospace Engineering,
University of California, San Diego
9500 Gilman Dr., 92037-0411 La Jolla, CA, USA
fjrodriguez@ucsd.edu

ABSTRACT

The flow near the leading edge of a deep-water hydraulic jump has been studied experimentally. Measurements of the instantaneous velocity field show that this flow shares some important features with the well known mixing layer separating two streams with different velocities. Namely, the constant convective velocity of the large coherent structures found in the flow, the linear relation between their size and downstream position and a collapse of the self-similar behavior of the dimensionless mean velocity profiles. However, some interesting differences arise. On the one hand, the convective velocity of the large eddies is much slower than what would be expected in a mixing layer, due to the effect of the hydrostatic pressure. Furthermore, the measured value of the numerical constant relating growth rate and convective velocity is slightly larger than the values reported in the classical literature for mixing layers.

INTRODUCTION

The entrainment of air bubbles in strong hydraulic jumps or turbulent breakers is a phenomenon of interest in a wide range of applications, from aeration of flow in dam spillways to the formation of bubbly wakes in ships. It is, however, far from being fully understood. The key difficulty is that the flow field close to the leading edge, or toe, where most of the entrainment occurs, is not easy to characterize using conventional measurement techniques in fluid mechanics nor is it easy to study using well established analytical or numerical tools. As an example, high void fraction together with large bubble sizes make classical optical velocimetry techniques inadequate for the study of the flow in the region of main interest.

It is commonly accepted that near the leading edge of a turbulent bore, where the high-speed stream impinges into a region of slower and deeper fluid, an unsteady two dimensional shear layer between the upper (nearly stagnant) and lower (fast) streams is formed. This mechanism was first clearly stated by Peregrine & Svendsen (1978). Moreover, they also pointed out that even in hydraulic jumps, where the bottom of the channel is close enough to affect the overall flow field, the initial development of this mixing layer may be considered to be free of this effect. This idea was further advanced by Hoyt & Sellin (1989), who investigated various similarities between the hydraulic jump and the mixing layer. They found linear growth of the coherent structures, with a strong asymmetry between the fast and slow streams. Unfortunately, they performed only a limited set of measurements of the spread angle and no measurements of the velocity field, so very little quantitative information can be drawn from their results. Accurate experimental characterization of the instantaneous velocity field in the shear layer found in a weak spilling breaker was obtained by Lin & Rockwell (1994) from PIV measurements. This technique allowed them to clearly identify large coherent structures developing between the high speed stream and the spilling water mass. More recently Liu, Rajaratnam & Zhu (2004) used Doppler Ultrasound Velocimetry to characterize the turbulent stresses in low Froude number hydraulic jumps, where the void fraction is small enough for this technique to operate properly. These authors found a peak in the shear Reynolds stress at the center line of the mixing layer, where turbulent intensities of more than 20% are reported. More interestingly, they also found that these stresses exhibit a self-similar profile.

On the other hand, some researchers have focused on the direct measurement of the void fraction and bubble distribution in hydraulic jumps using pitot tubes, and conductivity or optical probes, (Chanson & Brattberg, 2000, Murzyn *et al.*, 2005). The void fraction distribution that they measure corresponds fairly well with that expected in a two-phase shear layer. Nevertheless, the structure of the turbulent velocity field is not addressed in these studies.

In the present work, the structure of the mixing layer developing from the leading edge of a turbulent hydraulic jump is experimentally studied, with the aim at characterizing the dynamics of the large coherent structures found in the flow. Furthermore, the structure of the mean velocity field will be investigated, pointing out some similarities and differences with classical shear layers. To the best of our knowledge, this is the first time that such studies are performed in hydraulic jumps with high void fractions, where conventional velocimetry techniques fail to yield reliable results.

It is worh mentioning that, since this investigation deals with the dynamics of the flow in the entrainment region where bottom effects are negligible, the conclusions that will be obtained are applicable to other entraining flows such as breaking waves and turbulent bores.

EXPERIMENTAL SET-UP

The experiments were carried out in a recirculating water channel with a capacity of roughly five cubic meters. The test section is 2 m long and has a square cross section of 0.6 m x 0.6 m. The channel has a series of grids and honeycombs, followed by a contraction, to assure that fluctuations originating at the pump are damped out before the flow reaches the test section. The underlying turbulent intensity of the free stream is very low, less than 0.5%. A plexiglass plate was cut to dimensions 0.6 m x 0.0127 m x 1 m and fixed to supports so it could be placed vertically across the test section of the water channel. An auxiliary plate was

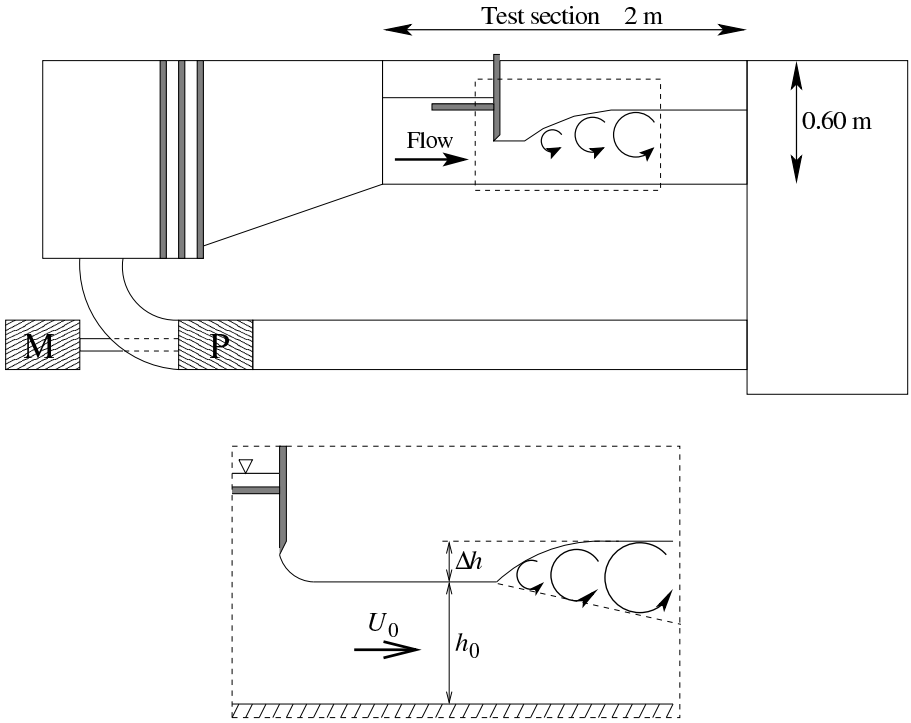

Figure 1: Sketch and detail of the experimental facility.

located horizontally along the channel at a low depth under the free surface upstream of the jump. In this way, the surface oscillations and spurious bubbles entrained upstream of the region of interest were avoided. Once positioned inside the test section, the flat plate extended through the entire width of the test section, from a distance of about 0.2 m (depending on the experimental session) from the bottom of the channel to well above the free surface. The end of the sluice gate that induces the hydraulic jump was machined to a sharp edge so that the free stream detaches cleanly from the gate without any possible boundary layer growth that would perturb the experiment and hinders its reproducibility. For each experimental session, the free stream velocity was measured using a pitot tube. It must be pointed out that the velocity of the free stream was measured at different locations under the region of interest to check that it was kept almost constant, thus allowing us to discard any possible effect of the bottom in the dynamics of the large coherent structures. A sketch of the facility, as well as a detailed picture of the free stream initiated at the sharp edge, are shown in figure 1.

Flow visualization technique

Light scattered by the air bubbles entrained by the flow was captured by a Kodak ES 1.0 (1 Mpixel) digital camera at 180° collection angle (first mode reflection). Illumination was provided by a strobe light positioned nearly coaxial with the optical axis of the camera. The camera was focused in a very narrow vertical plane aligned with the mean direction of the flow and located a few centimeters from the channel walls. Thus, the behaviour of the flow and the bubbles in a characteristic plane away from the influence of the boundaries was measured and analyzed.

In order to obtain as much information as possible on the dynamics of the large coherent structures, correlation algorithms commonly used in particle image velocimetry (PIV) were applied to the analysis of image pairs of the hydraulic jump acquired Δt = 1ms apart. The synchronization of the camera and the strobe light was performed with a Real-Time Linux (RTAI) PC, which allows for accurate control of the timing. This technique, referred to as Bubble Image Velocimetry (BIV, Ryu *et al.* 2005), is able to detect, although with some limitations, the rolling motion of the cloud of bubbles entrained by the large eddies, thus allowing the measurement of the velocity field wherever the bubble concentration field is such that there are more than a few bubbles in the interrogation window. It must be pointed out that due to the nature of BIV, it is not suited to characterize the fine scale velocity fluctuations of the flow. Therefore, the size of the interrogation window was chosen to be relatively large in order to average these small scale fluctuations. Thus, the velocity measurements correspond only to the velocity field associated with the large scale eddies in the flow. All the experimental results described in this paper were obtained with an interrogation window of 64×64 pixels with a 50 % overlap, which provided for about 10 velocity measurements along the diameter of a large eddy.

Vortex detection technique

Although numerous techniques to determine the position of the centre of a vortex are available in the literature, most of them require the calculation of the spatial derivatives of the velocity field. Unfortunatelly, the BIV technique used does not provide the spatial resolution necessary to allow for the application of any of those techniques. However, in the case under consideration it is possible to take advantage of the slender nature of the flow to carry out the detection using an algorithm that involves integration of the velocity field rather than differentiation. Similarly to what happens in a classical mixing layer, the centres of the large eddies lay along a line that is nearly parallel to the free stream, which coincides with the horizontal direction in the present flow. Thus, when evaluated along this line, the vertical velocity is expected to experience a change in sign precisely at the

Table 1: Experimental conditions. As sketched in figure 1, U_0 and h_0 are the free stream velocity and water depth upstream of the jump whereas Δh is the height jump. On the other hand, $u_{\min}$ is the minimum mean horizontal velocity measured in the flow, that corresponded to that at the top of the "roller".

Session	U_0 (m/s)	$u_{\min}$ (m/s)	h_0 (m)	Δh (m)
1	2.48	-0.29	0.115	0.151
2	2.21	-0.19	0.098	0.144
3	2.07	-0.04	0.150	0.110

centre of every vortex. Moreover, since the sense of rotation of the vortices must always be counterclockwise, this change in sign must be from negative to positive values as we move towards increasing values of x. To simplify the detection process and to make it more robust, the vertical velocity along x-stations is integrated. The change in sign of this integral quantity corresponds to the downstream position of the vortex centre. An example of the detection performed with this criterion is shown in figure 2. The upper part of the figure is a snapshot of the flow with the velocity vectors overimposed. The lower graph shows the value of the average vertical velocity for constant x stations together with the detected positions of the vortices marked with circles. Finally, in order to avoid spurious zero-crossings of the average vertical velocity to be taken as vortices, the detected positions were visually inspected and, when the detection was not successful, they were removed from the data.

EXPERIMENTAL RESULTS

Three experimental conditions, summarized in table 1, have been studied following the procedure described in the previous section. The analysis of the instantaneous velocity fields obtained through BIV reveals the existence of large coherent vortices already described in the literature for both hydraulic jumps and spilling breakers, Hoyt & Sellin (1989), Lin & Rockwell (1995), Svendsen, Veeramony, Bakunin & Kirby (2000). Nevertheless, to our best knowledge no quantitative description of the dynamics of these structures has been published. An interesting feature of these vortices, is that they exhibit a nearly constant convective velocity, at least within the measurement region. In figure 3, the time evolution of the position of the centres of the large vortices is shown for the three experimental sessions available. From the $x-t$ trajectories of the centres, the mean convection velocities of the vortices for the three sessions can be measured, obtaining $u_c = 0.71 \pm 0.14$ m/s, $u_c = 0.59 \pm 0.16$ m/s and $u_c = 0.72 \pm 0.14$ m/s respectively. This constant velocity resembles the behaviour observed for the large coherent structures in a classical mixing layer. However, some interesting differences arise. The first one is that the measured convective velocities do not correspond to the average speed between the maximum and the minimum measured in the flow, which for this particular flow would correspond to the velocities of the free stream and the spilling mass of fluid close to the free surface, respectively. Also, in parallel to what happens in stratified mixing layers between fluids of different densities in the presence of gravity, very few pairing events between consecutive eddies are observed. These two effects will be discussed in more detail in the next section.

This mixing-layer-like behaviour of the flow near the toe of the jump is not incompatible with the classical picture of a roller structure. The streamlines computed for the mean velocity field of sessions 1 and 3 are presented in figure 4. The streamlines for session 2 are not shown, as they are very similar to the result from session 1. The roller, or recirculation region, can be observed in these representations of the average velocity. Moreover, the mean velocity field can also be used to characterize the growth rate of the mixing layer. This is preferable rather than measuring the visual thickness based on the size of the large vortices, as this last technique has proven to be too sensitive to the illumination conditions. Therefore, to charaterize the growth rate of the mixing layer, a dimensionless horizontal velocity will be defined as

$$U = \frac{u - u_{\min}}{U_0 - u_{\min}} \tag{1}$$

with $u_{\min}$ being the minimum horizontal velocity measured in each experimental session, which corresponds to that of the spilling fluid close to the free surface. The growth rate will be defined from the separation between iso-lines $U(x, y_{0.1}) = 0.1$ and $U(x, y_{0.35}) = 0.35$ respectively. These values have been chosen as far as possible from each other but without entering into regions too close to the free surface or to the lower limit of the shear layer, where measurements are noisier. In figure 5, lines $y_{0.1}$ and $y_{0.35}$ corresponding to the three experimental sessions are shown. The existence of a region where the mixing layer grows linearly can be clearly observed. The tangents of the spread angles in the linear-growth region for the three sessions are $\delta = 0.125$, $\delta = 0.123$ and $\delta = 0.110$. Furthermore, comparison with figure 4a indicates that the linear growth occurs in a region that corresponds fairly well with the roller.

At this point, it is tempting to plot the profiles of the dimensionless velocity, $U(x, y)$, for different x stations within the region of linear growth versus a dimensionless vertical coordinate defined as $\eta = (y - y_{0.1}) / (y_{0.35} - y_{0.1})$, looking for some kind of self-similarity. This is done in figure 6. Indeed, all the velocity profiles seem to collapse into a single curve for a reasonably wide range of the dimensionless vertical coordinate, η. This self-similar behaviour is partially represented by the error function, as suggested by Townsend (1976) for the velocity profiles in a classical shear layer. The measured dimensionless velocity profiles are not antisymmetric, however, in a departure of the dynamics of this flow with the canonical shear layer.

ANALYSIS AND DISCUSSION OF THE RESULTS

As shown in the previous section, the flow in the proximity of the toe of a strong hydraulic jump shares some features with the classical shear layer described in the literature, namely the existence of large coherent vortices that are convected downstream, the linear growth of the layer (and therefore of these large vortices) and the collapse of the horizontal velocity profiles, when properly made dimensionless, into a self-similar profile. Nonetheless, when quantitative results of the measurements are compared with predictions made using the classical shear layer theory, some interesting differences arise.

Convective velocity of the large eddies

The first difference concerns the convective velocity of the large coherent structures, u_c. Indeed, the measured velocities are notably lower than the value predicted for a shear layer developing between two streams with velocities U_0 and $u_{\min}$ respectively, that it would be $u_c^{SL} = (U_0 + u_{\min})/2$ or, making u_c^{SL} dimensionless through expression (1), $U_c^{SL} =$

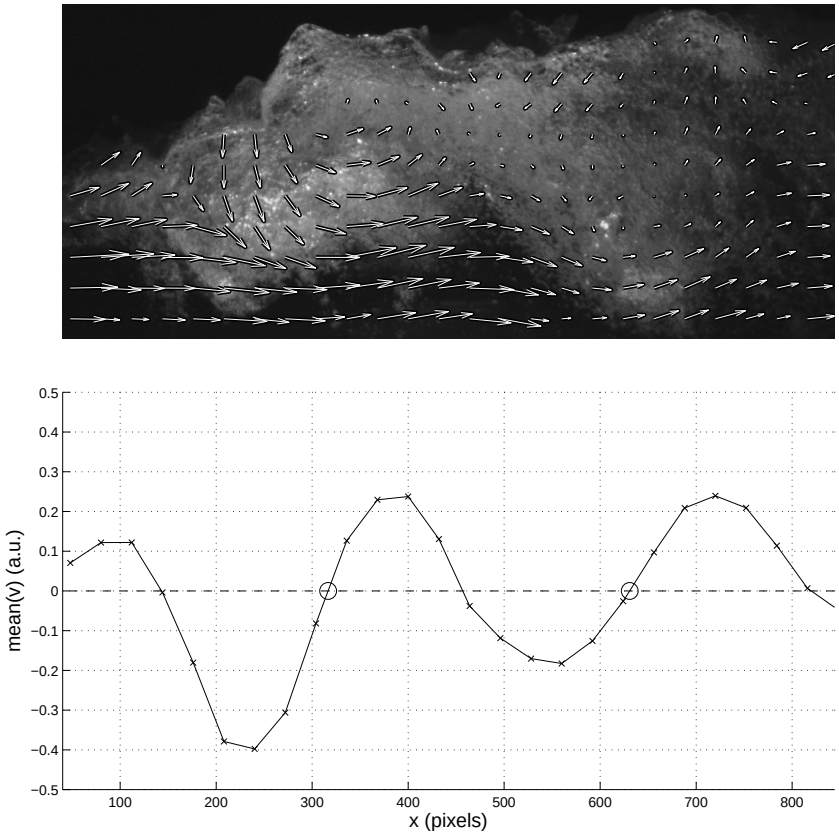

Figure 2: Example of vortex detection. At the top, a flow image, with the velocity vectors obtained from BIV, is shown. In the lower plot, the mean vertical velocity at each x-station is shown, with the circles representing the horizontal positions of the vortices detected by the algorithm.

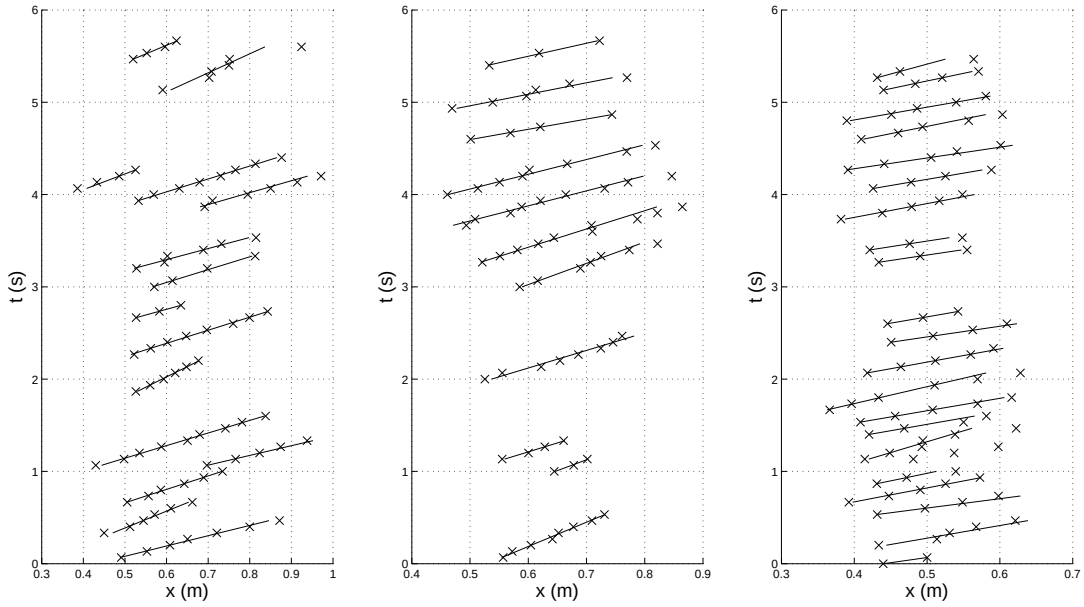

(a) (b) (c)

Figure 3: $x - t$ graph showing the time evolution of the position of the centres of the large eddies for sessions 1 (a), 2 (b) and 3 (c).

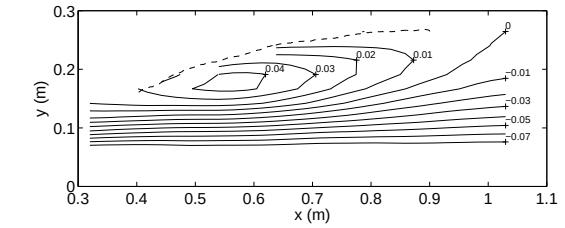

(a)

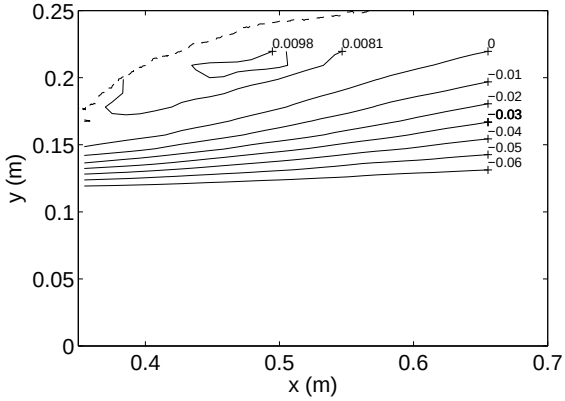

(b)

Figure 4: Streamlines and velocity vectors of the average velocity field corresponding to experimental sessions 1 (a) and 3 (b). The dashed line corresponds to the average position of the free surface.

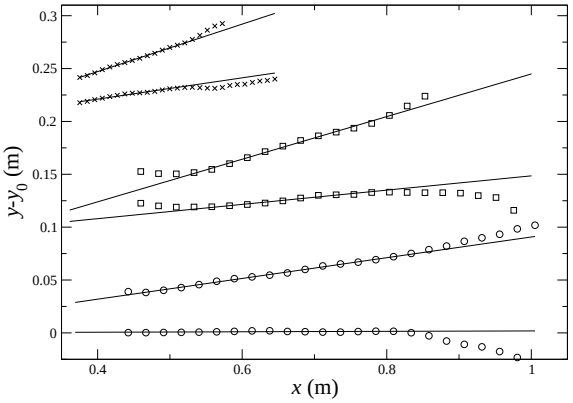

Figure 5: Lines corresponding to dimensionless horizontal velocities equal to 0.1 (upper) and 0.35 (lower) for sessions 1 (circles), 2 (squares) and 3 (crosses). Vertical coordinates are refered to the height of the virtual origin, y_0, and sessions 2 and 3 have been shifted 0.1 m and 0.2 m respectively for clarity.

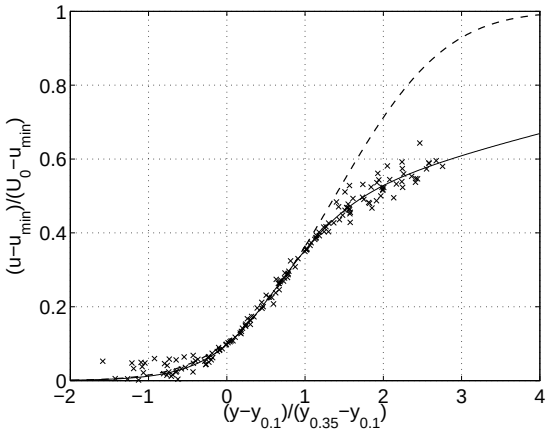

Figure 6: Dimensionless velocity profiles within the region of linear growth for the three sessions. The solid line corresponds to the fitting curve $U = (1+\tanh(1.085(\eta-0.561)))(1+\tanh(0.125(\eta-1.178)))/4$, whereas dashed line is given by a function of the form $U = \left(1+\mathrm{erf}\left((\eta-\eta_0)/\sqrt{2}C\right)\right)/2$, as suggested by Townsend (1976).

0.5. Instead, the measured dimensionless convective velocity is $U_c = 0.35$. To explain this lower velocity, a reasoning similar to the one used by Dimotakis (1986) is followed. In a galilean reference frame moving downstream with speed u_c, such that the large vortices lay at rest on it, a stagnation point must exist between two consecutive eddies (point C in figure 7). Assuming irrotational flow outside the vortices and neglecting unsteady effects, Bernoulli equations can be applied between point C and points A and B corresponding the former to a point at the free surface upstream of the toe and the latter to the position where the minimum horizontal velocity is found (see figure 7). Combining Bernoulli equations between points $A-C$ and $B-C$ respectively yields

$$\frac{1}{2}\rho\left(u_{\min}-u_c\right)^2+\rho g\Delta h=\frac{1}{2}\rho\left(U_0-u_c\right)^2 \qquad (2)$$

An extra simplification has been to assume that point B is at a height Δh over the upstream free surface. Now, the convective velocity, u_c, can be isolated from the above equation, resulting

$$u_c=\frac{U_0+u_{\min}}{2}-\frac{g\Delta h}{U_0-u_{\min}} \qquad (3)$$

Substituting into equation (3) the values corresponding to the three experimental sessions, the following values are obtained for the predicted convective velocities: $u_c^{\mathrm{P}} = 0.56, 0.42$ and 0.50 m/s. Although these values are much closer to the measured ones than those obtained without accounting for the effect of the height difference, Δh, still they exhibit some differences. The main reason for this, is that the height difference between the layer where the minimum velocity is found and that where the centres of the vortices lay is actually smaller than Δh.

To conclude this subsection, it is worth mentioning that the measured value of the dimensionless horizontal velocity ($U_c = 0.35$) is nearly that corresponding to the inflexion point of the self-similar velocity profile, as inspection of figure 6 reveals. This seems to indicate that the large coherent structures form at the position where the turbulent shear stress is maximum, as could be expected. However, due to the lack of antisymmetry exhibited by the velocity profiles,

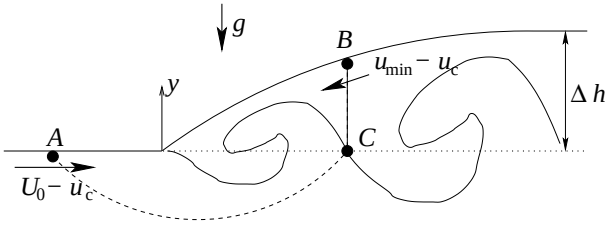

Figure 7: Sketch of the flow field with the paths used to apply Bernoulli equation.

in the present flow this does not occur at the vertical position where the average velocity between both streams is found.

Growth rate

As mentioned above, very few pairing events between consecutive eddies were observed. Therefore, engulfment of irrotational fluid analogous to the one described by Dimotakis (1986) and Hernan & Jimenez (1982), among others, emerges as the mechanism responsible for the growth of the shear layer. In order to compare with results available in the literature, a vorticity thickness can be calculated

$$\delta_\omega = \frac{U_0 - u_{\min}}{|\partial u/\partial y|_{\max}} \tag{4}$$

Using the curve corresponding to solid line in figure 6 to evaluate the derivative of the velocity profiles, the vorticity thickness may be related with the measured one, $\delta = y_{0.1} - y_{0.35}$, resulting $\delta_\omega = 3.78\,\delta$. The values thus obtained for the three sets are $\delta_\omega = 0.472, 0.465$ and 0.415. It is well known that in a shear layer, the thickness must be related to the maximum velocity difference, $\Delta U = U_0 - u_{\min}$, and the convective velocity of the large eddies, u_c in the following way

$$\frac{\mathrm{d}\delta_\omega}{\mathrm{d}x} = \alpha \frac{\Delta U}{u_c}, \tag{5}$$

where α is a constant that, for this particular flow, takes the value $\alpha = 0.124 \pm 0.017$. It is interesting to notice that the value suggested by Dimotakis (1986), $\alpha_D \approx 0.085$, is smaller than the one obtained here. This fact is consistent with the non-antisymmetric behavior of the velocity profiles. Indeed, $\alpha\Delta U$ is related to the turbulent intensity found in the flow, which in a mixing layer with zero-pressure-gradient, is about 17% of the maximum velocity difference, ΔU (Townsend, 1976), whereas in the hydraulic jump this value is larger (Liu, Rajaratnam & Zhu, 2004). However, as pointed out also by Townsend (1976) (section 6.10), a relatively small turbulent intensity is required in order for the velocity profile to be antisymmetric. Thus the non-antisymmetry of the velocity profiles may be associated to higher values of the turbulent intensity.

CONCLUSIONS

The flow near the leading edge of a deep-water hydraulic jump has been characterised using bubble image velocimetry. This technique has been used to study the dynamics of the large coherent vortices whose existence, for this kind of flows, is widely reported in the literature. Indeed, measurements show that the flow in this region not only resembles the well known mixing layer separating two infinite streams with different velocities, but also shares a number of common features from the quantitative point of view.

First, the large coherent vortices are convected downstream at a nearly constant speed. However, this convective velocity does not correspond to the mean value between the maximum and the minimum horizontal velocities found in the flow, as is the case in a mixing layer. Rather than that, it has been showed that proper computation of the convective velocity requires taking into account the effect of the hydrostatic pressure.

Second, the shear flow under study, and therefore the large eddies, grow linearly with the downstream distance, although the measured values of the growth rate are slightly greater than those reported in the literature for a mixing layer. Regarding the growth mechanism of this shear flow, very few pairing events, or amalgamations, have been observed. Therefore it can be concluded that the eddies grow due to the engulfment of irrotational fluid.

Furthermore, when properly made dimensionless, the mean velocity profiles exhibit a self-similar behavior within the region of linear growth. This self-similar velocity profile is not antisymmetric with respect to the point of maximum shear stress or, equivalently, the inflexion point. On the contrary, it approaches the free stream velocity more slowly than what would be expected in a mixing layer. This lack of antisymmetry is indicative of a larger value of the turbulent intensity that would also be consistent with the larger values of the growth rate measured.

REFERENCES

Chanson, H. & Brattberg, T. 2000 Experimental study of the air-water shear flow in a hydraulic jump. Int. J. Multiphase Flow 26 (4), 583607.

Dimotakis, P. E. 1986 Two-dimensional shear-layer entrainment. AIAA J. 24 (11), 17911796.

Hernán, M. A. & Jiménez, J. 1982 Computer analysis of high-speed film of the plane turbulent mixing layer. J. Fluid Mech. 119, 323345.

Hoyt, J. W. & Sellin, R. 1989 Hydraulic jump as a mixing layer. J. Hydr. Res. 115 (12), 16071614.

Lin, J. C. & Rockwell, D. 1994 Instantaneous structure of a breaking wave. Phys. Fluids 6 (9), 28772879.

Lin, J. C. & Rockwell, D. 1995 Evolution of a quasi-steady breaking wave. J. Fluid Mech. 302, 2944.

Liu, M., Rajaratnam, N. & Zhu, D. Z. 2004 Turbulence structure of hydraulic jumps of low froude number. J. Hydr. Eng. 130, 511520.

Murzyn, F., Mouaze, D. & Chaplin, J. R. 2005 Optical fibre probe measurements of bubbly flow in hydraulic jumps. Int. J. Multiphase Flow 31, 141154.

Peregrine, D. H. & Svendsen, I. A. 1978 Spilling breakers, bores and hydraulic jumps. Proc. 16th Int. Conf. Coastal Engng. Hamburg 1, 540550.

Ryu, Y., Chang, K. A. & Lim, H. J. 2005 Use of bubble image velocimetry for measurement of plunging wave impinging on structure and associated greenwater. Meas. Sci. Tech. 16, 19451953.

Svendsen, I. A., Veeramony, J., Bakunin, J. & Kirby, J. 2000 The flow in weak turbulent hydraulic jumps. J. Fluid Mech. 418, 2557.

Townsend, A. 1976 The structure of turbulent shear flows. Second edition.. Cambridge University Press.